

# Research on Electromagnetic Suspension (EMS) Control Method Based on Force Balance

Xu Junqi, Zhou Yuan, Wu Xiaodong, Rong Lijun, Qu Tao

Shanghai Maglev Transportation Engineering R&D Center, Longyang Road 2520, Shanghai 201204, P.R.China

nmtcxjq@163.com, coatpig@126.com

**ABSTRACT:** Due to the inherent nonlinearity and open-loop instability of EMS system, a new nonlinear control method based on force balance is proposed in this paper, and with a bi-DSP suspension controller designed, this nonlinear control method is implemented on the Shanghai Urban Maglev Test Line(SUMTL) and the tests are performed for making an experimental comparison with the classic control method based on PID algorithm. The effectiveness and feasibility of the proposed method is validated by experimental result.

## 1. INTRODUCTION

As Electromagnetic Suspension (EMS) system is nonlinear and open-loop unstable, it is usually linearized around the equilibrium point to build a linear model, and based on this linear model a classic state-feedback method is designed for suspension control, such as PID control. However, it is experimentally found that the performance apparently goes bad when the operating state is far from the equilibrium point.

In this paper, a nonlinear control algorithm for suspension is proposed. Furthermore, with a bi-DSP suspension controller designed, this new control method is implemented on the Shanghai Urban Maglev Test Line(SUMTL), and its performance compared with the traditional PID method verifies the effectiveness and feasibility of the new nonlinear suspension control method.

## 2. NONLINEAR FEEDBACK-LINEARIZING MATHEMATIC MODEL BUILD

EMS system generally consists of several electromagnet modules, and each module's movement system has 6 degree-of-freedom including: lift, lateral and longitudinal motion, rolling, pitch and yaw. By mechanically decoupling,

EMS system control can be decomposed into a single electromagnet module control unit. It is more practical to analyze the characteristic of single electromagnet suspension system than multi-electromagnet coupling system. Actually, the bogie and carriage of maglev train are connected by air-spring (called secondary spring), and due to the wide difference between inherent frequency of secondary spring and spectrum of suspension close-loop control system, the effect of secondary spring to system dynamic performances could be ignored; and the deformation response of vehicle-guideway is treated as disturbance force. A simplified single-electromagnet suspension system module is illustrated in fig.1 as follows.

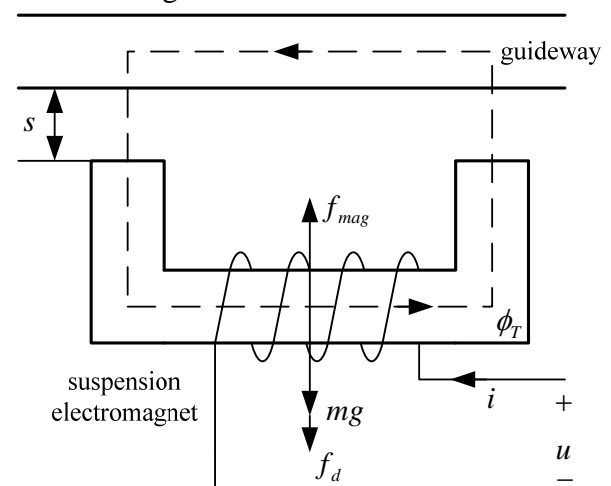


Fig.1 single-electromagnet suspension system module

Where  $m$  is gross mass of bogie, carriage, load and electromagnet;  $i$  is electromagnet coil current;  $s$  is suspension airgap;  $u$  is electromagnet coil voltage;  $f_{mag}$  is suspension force produced by electromagnet; and  $f_d$  is disturbance force.

With the relationship between voltage and current of electromagnet considered and assumed positive direction is vertical upward, the dynamic equation for the single-electromagnet suspension system is given as follows:

$$\begin{cases} m\ddot{s} + f_{mag} = mg + f_d \\ u = Ri + 2ki\dot{s} - 2kis/s^2 \\ f_{mag} = k\left(\frac{i}{s}\right)^2 \end{cases} \quad (1)$$

Where the symbol  $k = \mu_0 N^2 A / 4$  is electromagnet constant;  $N$  is number of turns;  $A$  is valid pole area of coil;  $R$  is coil resistance;  $\mu_0$  is permeability of air.

### 3. NONLINEAR CONTROL ALGORITHM DESIGN BASED ON FORCE BALANCE

Fig.1 shows that equation (1) expresses the motion characteristic of electromagnet. Normally, the value of airgap  $s$  can be directly derived from eddy-current sensor, and the value of coil current  $i$  from Hall-type sensor. So the three state variables, i.e. airgap  $s$ , current  $i$  and airgap differential  $\dot{s}$  are chosen as control variables and set as follows:

$$x_1 = s, x_2 = \frac{dx_1}{dt}, x_3 = i$$

Substituted into equation (1), the nonlinear state-equation become:

$$\begin{bmatrix} \dot{x}_1 \\ \dot{x}_2 \\ \dot{x}_3 \end{bmatrix} = \begin{bmatrix} x_2 \\ -\frac{k}{m} \left(\frac{x_3}{x_1}\right)^2 + g \\ \frac{x_2 x_3}{x_1} - \frac{R}{2k} x_3 x_1 \end{bmatrix} + \begin{bmatrix} 0 \\ 0 \\ \frac{x_1}{2k} \end{bmatrix} u + \begin{bmatrix} 0 \\ \frac{f_d}{m} \\ 0 \end{bmatrix} \quad (2)$$

When high-speed current close-loop control is applied, the damping effect of coil inductance to current dynamic response can be ignored, and the above equation (2) can be simplified:

$$\begin{bmatrix} \dot{x}_1 \\ \dot{x}_2 \end{bmatrix} = \begin{bmatrix} x_2 \\ -\frac{k}{m} \left(\frac{i}{x_1}\right)^2 + g + \frac{f_d}{m} \end{bmatrix} \quad (3)$$

For linearization of system, the following notation is introduced:

$$z_1 = x_1 - s_0$$

$$z_2 = x_2$$

$$w = g - \frac{k}{m} \frac{1}{x_1^2} i^2 + \frac{f_d}{m} \quad (4)$$

Where  $s_0$  is nominal value of air gap at equilibrium point. Taking  $w$  as input of linear control system, and substituting (4) into (3), the equivalent linear open-loop model of equation (3) can be expressed as:

$$\begin{bmatrix} \dot{z}_1 \\ \dot{z}_2 \end{bmatrix} = \begin{bmatrix} 0 & 1 \\ 0 & 0 \end{bmatrix} \begin{bmatrix} z_1 \\ z_2 \end{bmatrix} + \begin{bmatrix} 0 \\ 1 \end{bmatrix} w \quad (5)$$

Equation (5) shows that the controllability matrix is full rank, so this open-loop system is controllable and can be stabilized by applying state-feedback control method. Introducing a control rule:  $w = -(k_1 z_1 + k_2 z_2)$  into equation (4), we can obtain the corresponding current control law:

$$i = x_1 \sqrt{\frac{mk_1 z_1 + mk_2 z_2 + mg + f_d}{k}} \quad (6)$$

Where the disturbance force  $f_d$  is calculated according to equation (1), and  $f_{mag}$  is calculated from  $f_{mag} = k(i/s)^2$  in equation (1) with the measure value of current  $i$  and airgap  $s$ .  $\ddot{s}$  can be obtained from accelerometer measure for the physical significance of  $\ddot{s}$  is acceleration  $a$  and gross mass  $m$  is a known quantity.

Recovering practical physical significance of the state variables, equation (6) can be written as follow:

$$\begin{aligned} f_{con} &= k \left(\frac{i}{s}\right)^2 \\ &= k'_1 (s - s_0) + k'_2 \dot{s} + f_d + f_0 = f_p + f_{ds} + f_d + f_0 \end{aligned} \quad (7)$$

Correspondingly, the variable of current control  $i_{con}$  is given by:

$$i_{con} = s \sqrt{\frac{f_{con}}{k}}$$

$$\text{where } k'_1 = \frac{mk_1}{k}; k'_2 = \frac{mk_2}{k}; f_0 = mg$$

Equation (7) shows that: electromagnetic force  $f_{con}$  should consist of the following parts:

i To make electromagnet work at stable point (practical airgap  $s$  at nominal value  $s_0$ ), the control force for eliminating the static error of airgap:  $f_p = k'_1 (s - s_0)$ .

ii The damping force for system from differential calculation of airgap:  $f_{ds} = k_2 \dot{s}$ .

iii To overcome the disturbance force, the anti-disturbance magnetic force: its value is equal to  $f_d$ .

These three forces is for dynamic adjustment, besides, the static magnetic force to overcome the weight ( $f_0 = mg$ ) of EMS system is necessary.

From the analysis, it is checked that only if the electromagnetic force balances the four forces illustrated above, the system can be approach to stability. The control diagram is shown in Fig.2, where  $i_1, a, s$  are input variables which can be measured directly,  $i_{con}$  is calculated control variable(the signal of desired current),  $k_1$  and  $k_2$  is variable parameter to adjust suspension stiffness and system damping.

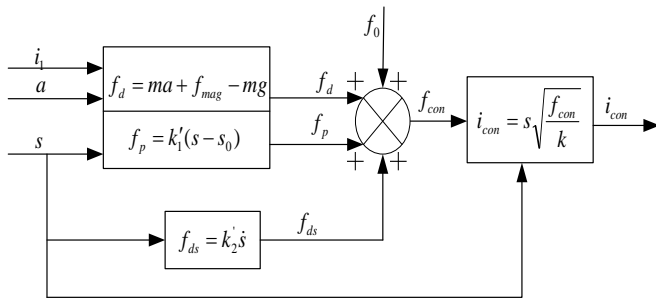


fig.2 control diagram based on force balance

#### 4. SIMULATION STUDY

The validation of the proposed nonlinear controller design is done by simulation study, the simulation result is compared with the traditional PID controller. The following physical parameters are chosen in this simulation:

$$m = 750kg, N = 340, R = 0.4, s_0 = 0.008m, A = 0.028 * 0.75m^2$$

Fig.3a shows the system response to an airgap step disturbance of 4mm (nominal airgap  $s_0$  is changed from 8mm to 12mm abruptly) when the system is in steady state, which is based on the classical PID controller.

Fig. 3b shows the system response to the same step disturbance, but for the proposed nonlinear controller.

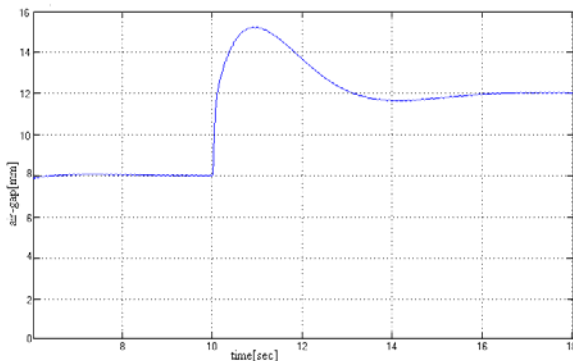


Fig.3a system step response for a PID controller

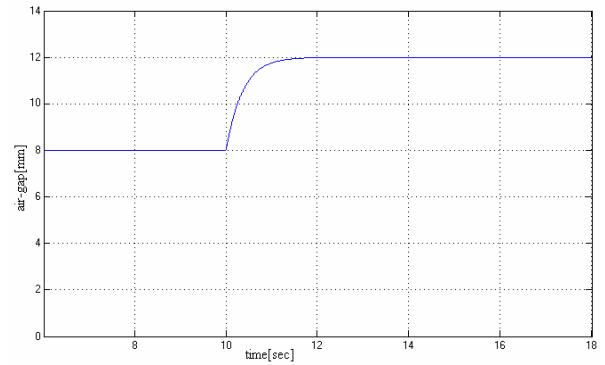


Fig.3b system step response for the proposed nonlinear controller

The simulation result shows that for a PID controller, the overshoot of system response to an airgap step disturbance is about 3mm, and transient time is 6s; however, for the proposed nonlinear controller based on force balance, there is no overshoot and transient time is within 2s. This simulation result verifies the proposed controller has a faster response and stronger robustness than the PID controller.

#### 5. EXPERIMENTAL CONFIGURATION

##### 5.1 Control Circuit Structure

The control circuit for the proposed control algorithm is constructed based on a bi-DSP structure shown in Fig.4 where the model of DSP1 and DSP2 is TMS320F2812. Double Port Random Memory chip realizes the parallel data communication between the two DSPs. The address logic among DSP1, DSP2 and peripheral chips is controlled by CPLD. The high-precision multi-parallel sampling A/D chip is extended. And CAN interface for communication between the suspension controller and upper computer is deployed. DSP1 performs sampling and filtering of the airgap, acceleration and current signal, and calculating the differential value of the airgap signal. Before sampled by A/D, the three signals need to be filtered through Analog Anti-aliasing Filter (AAF); DSP2 performs the proposed control algorithm based on balance force, calculates the desired value of current  $i_{con}$  and generates the PWM pulse control signal according to the desired current value  $i_{con}$ . In addition, DSP2 can communicate with upper computer through CAN interface to implement the setup of control parameters and the upload of state information.

The advantage of bi-DSP hardware structure is the high rapidity of sampling and follow-up processing, the decrease of signal delay, and the high efficiency of complicated calculation, such as nonlinear control algorithm, differential, square/extraction and scaling etc., which thoroughly

meets the request of rapidity and precision of the proposed control algorithm.

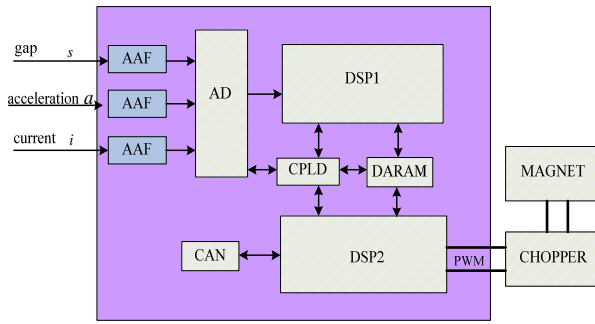


Fig. 4 block diagram for bi-DSP suspension control

### 5.2 Control Software

Control software includes two parts: signal processing software in DSP1 and control algorithm software in DSP2. With debugging experiences, we setup the interruption cycle of DSP1 and DSP2 is respectively 100us and 500us, which leads to satisfactory performance of suspension control.

## 6. EXPERIMENTAL RESULT

With the designed suspension controller, the suspension and propulsion experiment is carried out on the maglev train at SUMTL. This maglev train consists of three sections and each section is supported by five suspension bogies. At the each side of a suspension bogie, one suspension electromagnet is assembled separately, and each electromagnet has two control circuits, which are controlled by two of the designed controllers. So, there are twenty suspension controllers in one section. Fig.5 shows the maglev train on the SUMTL. In the experiment, the 3-section train can stably go through those critical track segments with 50m horizontal curve, 70m horizontal curve, 1500m vertical curve, and the steel guideway switch. The maximal speed of the train is 100km/h and the suspension fluctuation is within  $\pm 2$ mm.



Fig. 5 The maglev train on SUMTL

Fig.6~8 shows the curves of experimental data tested by a third party. Fig.6 shows the curve of airgap data of a suspension point at the speed of

90km/h, where the peaks of curve reflect the timing when the airgap sensor detects the guideway joint gaps. Fig.7 shows the curve of airgap data of a suspension point when the train is passing by the track of 70m horizontal curve at 35km/h with the proposed nonlinear controller installed, and for contrast, Fig.8 shows the curve of airgap data of a suspension points under the same working condition but with the traditional PID controller installed.

When the train is passing by curve, the excitation model is changed apparently due to the relative position deviation of electromagnet to “F” shaped track and the relative position change between the carriage and bogie leads to a biggish dynamic change of load at suspension point. So, we need the controller to regulate the electromagnet current quickly and precisely enough to adapt to the system parameters change for keeping the stable suspension. From fig.8, it is found that the traditional PID controller cannot real-time adjust the control variables corresponding to the change of system parameters, which brings the big airgap fluctuation about  $\pm 6$ mm and the system stability is damaged which leads the electromagnets and skids touch the “F” shaped track. However, under the proposed nonlinear control based on force balance, the real-time adjustment of control variables can be achieved, avoiding the big airgap fluctuation greatly(airgap fluctuation limited within  $\pm 2$ mm shown in fig.7), which shows the superiority of the proposed control method. The experiment result proves that the proposed nonlinear control can greatly improve the system robust and adaptability to guideway parameter change.

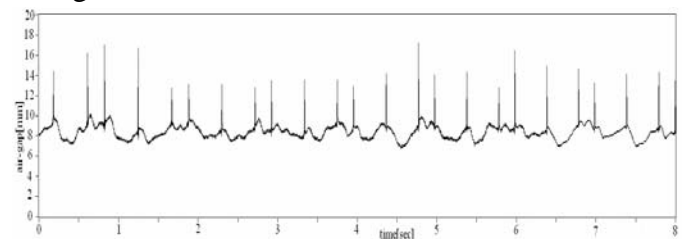


Fig.6 suspension airgap signal at 90km/h using the proposed nonlinear controller

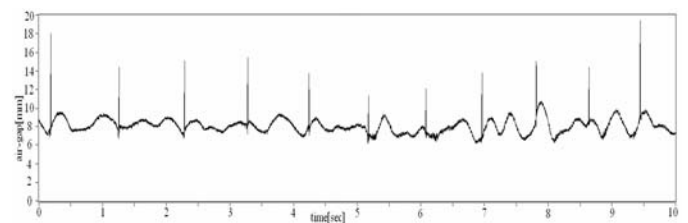


Fig.7 suspension airgap signal passing by 70m curve using the proposed nonlinear controller

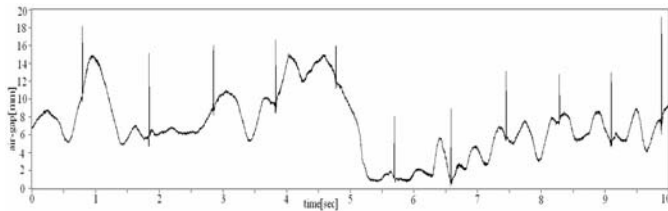


Fig.8 suspension airgap signal passing by 70m curve under PID control

## 7. CONCLUSION

Based on the dynamic model of single electromagnet EMS system, a nonlinear control algorithm based on force balance is proposed with practical physical significance of each control variable analyzed. And the simulation study of this proposed control is done. Furthermore, a bi-DSP suspension controller is designed and implemented according to this control algorithm, and the controller is applied on the maglev train on SUMTL. Running test and measurement prove the adaptability of this control method to all kinds of working conditions on the test line, this control method satisfies the needs of suspension control performance. Compared with the traditional PID control, the simulation and experimental result verifies the effectiveness and feasibility of this proposed control method which has a great significance for optimizing and improving the performance of suspension control system.

## 8. REFERENCES

- Liu Hengkun , Shi Xiaohong & Chang Wensen. 2007. Nonlinear Control of Maglev. *Systems Control Engineering of China* 14(5):455-457.
- Long Zhiqiang , Hong Huajie & Zhou Xiaobing. 2003 . Research of nonlinear control for maglev train. *Control Theory & Applications* 20(3):399-402.
- Jiang Hao & Lian Jisan. 1992.The Dynamic Model and Control of Single-magnet Suspension Systems. *Journal of Southwest Jiaotong University* 83(1):59-67 .
- Bao Jia & Zhang Kunlun. 2003. Research of Electromagnetic Suspension System of Single Magnetic. *Computer Automated Measurement & Control* 11(11):863-865.
- Deng Yunquan & Luo Shihui. 2005. Stability research and simulation of a single magnetic system. *Electric Locomotives & Mass Transit Vehicles* 28(5):44-46.
- SungJun Joo & Jin H. Seo, 1997. Design and Analysis of the Nonlinear Feedback Linearizing Control for an Electromagnetic Suspension System. *IEEE Transactions on Control Systems Technology* 17(5): 135-144.
- David L. 1997. Linearizing control of magnetic suspension systems. *IEEE Transactions on Control Systems Technology* 5(4): 427-438.